Stopped-Flow Analysis on Anion Binding to Blue-Form Halorhodopsin from *Natronobacterium pharaonis*: Comparison with the Anion-Uptake Process during the Photocycle[†]

Maki Sato,[‡] Tatsuaki Kanamori,[§] Naoki Kamo,[§] Makoto Demura,[‡] and Katsutoshi Nitta*[,‡]

Division of Biological Sciences, Graduate School of Science, and Graduate School of Pharmaceutical Sciences, Hokkaido University, Sapporo 060-0812, Japan

Received September 12, 2001; Revised Manuscript Received November 19, 2001

ABSTRACT: *pharaonis* halorhodopsin (*p*hR), the light-driven chloride ion pump from *Natronobacterium pharaonis* with C-terminal histidine tag, was expressed in *Escherichia coli* cells. The protein was solubilized with 0.1% *n*-dodecyl β-D-maltopyranoside and purified with a nickel column. Removal of Cl^- from the medium yields blue *p*hR (*p*hR^{blue}) that has lost Cl^- near the chromophore. Addition of Cl^- converts *p*hR^{blue} to a red-shifted Cl^--bound form (*p*hR^{Cl}). Circular dichroic spectra of *p*hR^{blue} and *p*hR^{Cl} exhibited a bilobe in the visual region, indicating specific oligomerization of the *p*hR monomers. The order of anion concentration which induced a shift from *p*hR^{blue} to *p*hR^{X} was $Br^- < Cl^- < NO_3^- < N_3^-$, which was the same as in the case of *p*hR purified from *N. pharaonis* membranes. Chloride binding kinetics was measured by time-resolved absorption changes with stopped-flow rapid mixing. Rates of Cl^- binding consisted of fast and slow components, and the amplitude of the fast component was about 90% of the total changes. The rate constant of the fast component at 100 mM NaCl at 25 °C was 260 s^{-1} with an apparent activation energy of 35 kJ/mol. These values are in good agreement with the process of Cl^- uptake in the photocycle (O → hR′ reaction) reported previously [Váró et al. (1995) *Biochemistry 34*, 14500−14507]. In addition, the Cl^- concentration dependence on both rates was similar to each other. These observations suggest that the O-intermediate is similar to *p*hR^{blue} and that Cl^- uptake during the photocycle may be ruled by a passive process.

Halorhodopsin (hR) in membranes of halobacteria is an electrogenic light-driven chloride pump from the extracellular to cytoplasmic side (*1*). Although numerous hRs have been identified and reported (*2*−*4*), the hRs that have been extensively studied so far are those from *Halobacterium salinarum* (*1*, *5*) and *Natronobacterium pharaonis* (*6*−*8*). The homology of the primary structure for both is very high (66%) (*9*). The structure of *H. salinarum* hR (*s*hR)[1] was recently solved by X-ray diffraction (*10*) at 1.8 Å resolution.

The spectral and kinetic studies clarified the following photocycle scheme of *p*hR: hR → K ↔ L ↔ N ↔ O ↔ hR′ → hR (*7*). In the case of *s*hR, the O-intermediate does not accumulate presumably for kinetic reasons (*11*). The release and uptake of Cl^- are associated with the N to O and the O to hR′ reactions, respectively. Furthermore, from the temperature dependences of rate constants, the photocycle of *p*hR was determined to be the thermodynamic cycle in which enthalpy−entropy conversion occurs in the O → hR′ reaction (*7*).

Absorption wavelength shift of hR by the binding of anions has been widely studied by various methods. The dependence of the absorption spectrum of *s*hR on the concentration of Cl^- (*12*) indicated a single Cl^--binding site. Studies using a spectroscopic method (*13*, *14*) and resonance Raman spectroscopy (*15*) have proposed two binding sites, of which one bound non-halide anions such as perchlorate near the Schiff base and the other bound halide in the retinal-binding pocket. In addition, a "one-site, two-state model" in which hR has a single tight binding site but two different conformational states has been proposed (*16*).

A ^{35}Cl NMR study revealed that *s*hR has two binding sites, one of which is different from the site in the vicinity of chromophore (*17*). Mutagenesis studies on *s*hR have revealed that the cytoplasmic pair R200/T203 was a candidate for the Cl^--binding site concerned with release (*18*). Also, Okuno et al. (*19*) postulated that *s*hR had three different Cl^--binding sites. For *p*hR, on the other hand, there is very little information on the binding site, although the effects of anions have been analyzed in detail using a spectroscopic method (*20*).

There are various advantages in using *p*hR. *pharaonis* hR has been reported to be more stable than *s*hR. Moreover, the retinal isomeric composition does not change by the condition of light/dark adaptation (*8*), and *p*hR transports

[†] The work was supported in part by a Grant-in-Aid from the Ministry of Education, Science, Sports, and Culture of Japan.

* To whom correspondence should be addressed. Telephone: +81-11-706-2773. Fax: +81-11-706-2771. E-mail: nitta@sci.hokudaia.ac.jp.

[‡] Graduate School of Science, Hokkaido University.

[§] Graduate School of Pharmaceutical Sciences, Hokkaido University.

[1] Abbreviations: CP, cytoplasmic channel; DM, *n*-dodecyl β-D-maltopyranoside; EC, extracellular channel; OG, *n*-octyl β-D-glucopyranoside; *p*hR, halorhodopsin from *Natronobacterium pharaonis*; *p*hR^{blue}, blue *p*hR that has lost Cl^- at the binding site near the chromophore; *p*hR^{X}, the anion- (X-) binding form of *p*hR; *s*hR, halorhodopsin from *Halobacterium salinarum*.

10.1021/bi011788g CCC: $22.00
Published on Web 01/24/2002

not only halide but also nitrate at about the same rate (*21*). Recently, the expression system of *Escherichia coli* of archaeal retinal protein was reported by Shimono et al. (*22*). Furthermore, the use of histidine-tagged protein makes it possible to purify *p*hR in only one step (*23*), thereby allowing simple and large-scale preparation.

In this paper, we expressed histidine-tagged *p*hR in *E. coli* and analyzed the binding affinities of various anions. Removal of anions from the medium yields a blue-shifted *p*hR (*p*hR^{blue}; maximum absorption wavelength, 599 nm) that has lost the anion near the chromophore. Addition of anions restores the anion-binding species (*p*hR^{X}; X denotes an anion) whose maximum wavelength is 578 nm (for Cl^-) or 577 nm (for Br^-). Analysis of the spectrum shift between *p*hR^{blue} and *p*hR^{X} gives the anion-binding affinity at equilibrium state. Using conventional stopped-flow techniques, time-resolved binding kinetics under various conditions are analyzed.

MATERIALS AND METHODS

Construction of the Expression Plasmid of the Histidine-Tagged Protein. The expression plasmid was constructed using the plasmid pET-21c(+) vector (Novagen, Madison, WI). To utilize the histidine-tagged region incorporated into the pET-21c(+) vector, the stop codon of the *p*HOP gene was deleted and the *Ava*I site was introduced into this site. The *p*HOP gene was amplified by PCR using template plasmid. PCR products were subcloned and restricted with the *Ava*I. This fragment was ligated into the pET-21c(+) vector. DNA sequencing was carried out using a DNA sequencing kit (Applied Biosystems, Foster City, CA). The sequence of histidine-tagged protein obtained by this method was

$$^{1}\text{MTETLP...TPADD}^{291}\textbf{LE}\text{HHHHHH}$$

The bold and underlined portions indicate a linker region and a histidine-tag region, respectively.

Protein Expression and Purification of phR. E. coli BL21-(DE3) cells containing the plasmid pET*p*hR were grown at 37 °C in 2 × YT medium supplemented with 50 μg/mL ampicillin. At an OD_{660} of 0.7−0.8, 1 mM IPTG (isopropyl 1-thio-β-galactoside) and 10 μM all-*trans*-retinal were added, and after 4 h cells were harvested. Cells were collected by centrifugation, suspended in buffer A [50 mM Tris-HCl (pH 8.0), 5 mM $MgCl_2$], and stored at −20 °C. Thawed cells were broken by a French press (Ohtake, Tokyo, Japan) at a pressure of 1200 kg/cm^2. Crude membranes were collected by centrifugation (106000*g* for 90 min at 4 °C). After being washed with buffer S [50 mM 2-morpholinoethanesulfonic acid, MES (pH 6.5), 300 mM NaCl, 5 mM imidazole], the crude membrane was resuspended in the same buffer, solubilized with 1.5% *n*-dodecyl β-D-maltopyranoside (dodecyl maltoside, DM) (Dojindo Lab, Kumamoto, Japan), and stirred for 14 h at 4 °C. After centrifugation (106000*g* for 90 min at 4 °C), the supernatant containing solubilized *p*hR was incubated with Ni-NTA−agarose (Qiagen, Hilden, Germany) for 1 h at room temperature. The NTA resin was applied to a chromatography column and washed with buffer W [50 mM MES (pH 6.5), 300 mM NaCl, 50 mM imidazole, 0.1% DM] to remove nonspecifically bound proteins. Fractions of *p*hR were collected by elution (flow rate, 56 mL/h) with buffer E [50 mM Tris-HCl (pH 7.0), 300 mM NaCl, 150 mM imidazole, 0.1% DM].

Preparation of the phR^{blue}. The anion-deleted blue species of *pharaonis* hR (*p*hR^{blue}) were prepared by interchanging with buffer C [10 mM 2-morpholinopropanesulfonic acid, MOPS (pH 7.0), 0.1% DM] in an Ultrafree-15 centrifugal filter device (Millipore, Bedford, MA). After the buffer exchange, the protein concentration was estimated using an excitation coefficient ϵ_{600} of 50000 $M^{-1}\cdot cm^{-1}$ (*20*).

Absorption and Circular Dichroic Measurements. Circular dichroic (CD) spectra of *p*hR were measured with a Jasco J-725 spectropolarimeter (Jasco, Tokyo, Japan) in the 300−750 nm region at 25 °C using a scanning speed of 200 nm/min and two accumulations. The measuring medium was buffer C containing various concentrations of NaX (with X = Cl^-, Br^-, NO_3^-, N_3^-). The protein concentration was 15 μM. The path length of the optical cuvette was 10 mm.

Absorption spectra were obtained by converting a photomultiplier voltage signal of a CD apparatus into the optical density (log I_0/I) using a computer. Since the samples do not show light/dark adaptation (*8*), no precautions were taken to bring to the light adaptation.

Time-Resolved Absorption Measurements. Time-resolved absorption changes caused by the rapid mixing of *p*hR^{blue} with NaX (X = Cl^-, Br^-) were measured using an RA-2000 stopped-flow spectrophotometer (Otsuka electronics, Osaka, Japan) with a dead time of 1.3 ms. The path length of the optical cell was 10 mm. The mixing volume ratio of the protein and the anion solutions was 1:1. The final protein concentration was 6 μM. Rapid scan absorption changes in the 520−700 nm range were collected using a photodiode array at 4 ms intervals after the mixing, which gave the difference spectra caused by the anion addition until 250 ms after mixing. The time-resolved absorption signal at fixed wavelength was collected using a photomultiplier at a sampling time of 0.2 ms, usually for 2 s.

RESULTS

Purification of the Histidine-Tagged phR. The mature *p*hR gene was amplified from plasmids containing the sequence of the wild-type proteins and ligated into the multiple cloning site of the *E. coli* expression vector pET-21c(+) together with oligonucleotides introducing a C-terminal histidine tag. Sequencing confirmed that no mutations occurred during PCR amplification. The purified histidine-tagged protein was characterized by SDS−PAGE and circular dichroic and absorption spectra (Figures 1 and 2; see also Table 1 for spectroscopic data). The absorption maximum (λ_{max}) of the recombinant *p*hR in the presence of Cl^- (*p*hR^{Cl}) was identified to be 578 nm, which was identical to those of the nonmodified protein purified from *N. pharaonis* membrane (*20*) and expressed in *E. coli* cells (recombinant *p*hR without the histidine tag) (data not shown). The protein purified from the native membrane is hereafter designated the authentic protein. The yield for histidine-tagged *p*hR calculated from the optical density at λ_{max} was 20 mg/L of cell culture.

Titration of phR^{blue} with Anions on Visible Circular Dichroic and Absorption Spectra. The Cl^--free form of *p*hR (*p*hR^{blue}) was titrated with NaCl. Circular dichroic (CD) spectra in the visible region (450−700 nm) exhibited a bilobe as shown in Figure 1, where the Cl^- concentration ranged

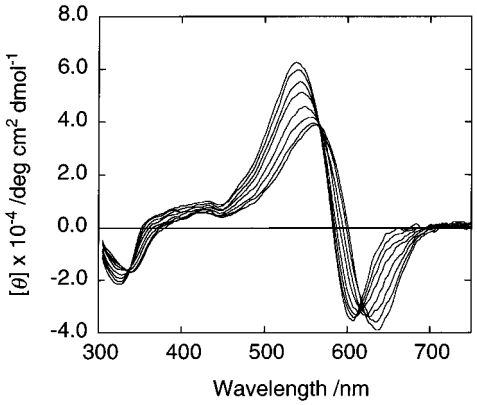

FIGURE 1: Circular dichroic spectra of *p*hR (15 μM) at various Cl^- concentrations. These spectra were taken in 10 mM MOPS (pH 7.0) and 0.1% DM. NaCl was added at a concentration of 0−200 mM. The volume changes due to the addition of concentrated NaCl solution were corrected. The measurement was carried out at 25 °C.

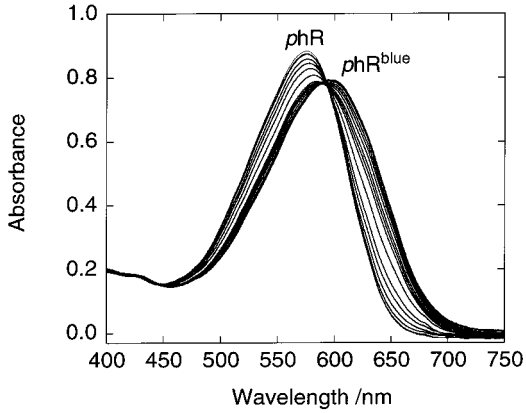

FIGURE 2: Absorption spectrum changes caused by the phR^{blue} → phR^{Cl} reaction. The experimental conditions were the same as those in Figure 1.

Table 1: Dissociation Constants (K_d), Hill Coefficients, and Absorption Maxima (λ_{max}) of phR^{blue} and phR^X at pH 7.0 and 25 °C[a]

salts	K_d/mM	Hill coeff	λ_{max}/nm
no addition			599
NaBr	8	1.3	577
NaCl	10	1.1	578
$NaNO_3$	43	1.6	571
NaN_3	63	1.6	568

[a] The dissociation constant and Hill coefficient were determined from the equation shown in the text by least-squares fits. Absorption maxima were measured at the plateau level of the absorption by the anion addition.

from 0 to 200 mM. A bilobe attributed to the intermolecular interaction between neighboring retinal molecules, known as an exciton interaction, indicates that recombinant *p*hR solubilized with DM is not a monomer but is associated, as has been observed in the authentic *p*hR solubilized with DM (*20*), *s*hR (*24*), and bR in the purple membrane (*25*). In the case of the Cl^--free condition, the exciton band of the CD spectrum of phR^{blue} is symmetrical with respect to the crossover point of the bilobe. With increasing Cl^- concentration, crossover points are blue shifted, and the positive exciton bands increased gradually. A similar dependence of CD spectra of the authentic *p*hR in the visible region has

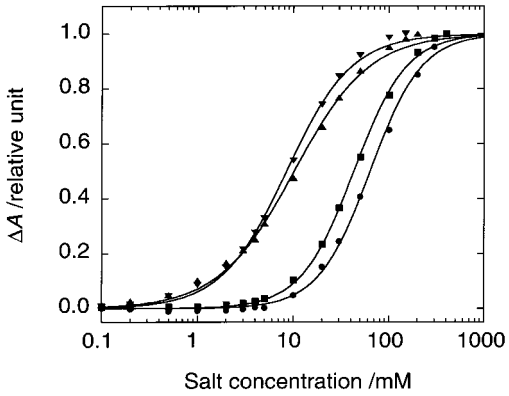

FIGURE 3: Absorbance changes vs salt concentrations during the phR^{blue} → phR^X reaction. The ordinate value was reduced by the maximum changes of respective anions: (▼) NaBr; (▲) NaCl; (■) $NaNO_3$; (●) NaN_3. phR^{blue} (15 μM) was solubilized in 10 mM MOPS (pH 7.0) and 0.1% DM, followed by the addition of various anions.

been reported (*20*). In addition, the blue shift of crossover points and the increase in the positive CD band of phR^X were also observed when X was Br^- or NO_3^-. On the other hand, only the blue shift of the bilobe was observed when N_3^- was used (data not shown).

Figure 2 shows absorption spectra in the range of 400−750 nm when titrated with Cl^- from 0 to 200 mM at pH 7.0. The isosbestic point was observed at 590 nm. The absorption maximum, λ_{max} of phR^{blue}, was 599 nm and that of *p*hR in the presence of 20 mM Cl^- was 578 nm. At higher ionic strength than 20 mM NaCl, no further shifts in the absorption maximum were observed.

Difference spectra induced by the anion addition calculated from Figure 2 (data not shown) showed the maximum changes at 633 nm, the same as that observed with a stopped-flow apparatus using a photodiode array (see Figure 4). Figure 3 shows the absorbance change at 633 nm as a function of anion concentration at pH 7.0. Upon addition of anions to phR^{blue}, the absorption changes (ΔA) follow sigmoidal curves with saturation, but their slopes depend slightly on the anion species. The values of ΔA were normalized by the saturation level. The apparent half-maximal binding concentration increased in the order of Br^- < Cl^- < NO_3^- < N_3^-. These saturation curves were fitted with the equation:

$$\Delta A = [\text{anion}]^n/(K_d{}^n + [\text{anion}]^n)$$

where K_d and n are the dissociation constant and Hill coefficient, respectively. The results are listed in Table 1. Values of K_d for Br^-, Cl^-, NO_3^-, and N_3^- were 8, 10, 43, and 63 mM, respectively. The Hill coefficients for all anions tested were approximately 1, but those for NO_3^- and N_3^- seemed slightly larger than unity. In the order of the K_d values, a result similar to that of the authentic *p*hR has been observed (*20*). However, slightly different K_d values for Cl^- have been reported for the authentic *p*hR (3 mM) and recombinant *p*hR in *H. salinarum* (∼1 mM) (*7*, *20*). The discrepancies might originate from the different sample preparation including heterologous expression system and different experimental conditions such as ionic strength.

Time-Resolved Absorption Changes by Rapid Stopped-Flow Mixing of phR^{blue}. The anion-binding kinetics of phR^{blue}

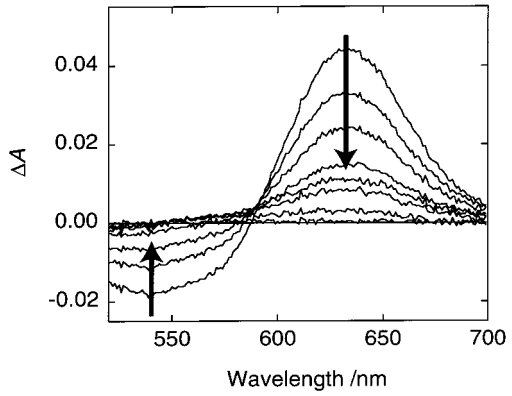

FIGURE 4: Time-resolved differential absorption spectra of the *p*hR^{blue} → *p*hR^{Cl} reaction. Proteins was solubilized in 10 mM MOPS (pH 7.0) containing 0.1% DM. The final concentrations of NaCl and the protein were 20 mM and 6 μM, respectively, and the reaction was carried out at 10 °C. Sixty-four spectra were collected every 4 ms, and representative spectra (4, 8, 12, 20, 36, 60, 100, and 250 ms after mixing) are shown. Arrows indicate spectral changes with increasing time.

was investigated using a stopped-flow apparatus. The *p*hR^{blue} was mixed with various concentrations of NaCl solution. Figure 4 shows the time-resolved differential absorption spectra when a NaCl solution was added to *p*hR^{blue} in the dark. As in the trial described above, a maximal absorption difference was observed at 633 nm. However, in this experimental condition, the difference spectra indicate an isosbestic point at 590 nm for only the earlier observed period. This fast decrease at 633 nm corresponds to the similar change at 550 nm. The following spectral decreases at 633 nm might not indicate the same isosbestic point, suggesting different kinetics between fast and slow processes. Thus, the time courses of absorption changes were measured at 633 nm, and the results are shown in Figure 5. When a single-exponential decay equation was applied, the residual between the best-fit curve and experimental data was large (inset of Figure 5A). Figure 5B and its inset show the best fit by assuming a two-exponential decay equation, and the rate constants were estimated to be 61 and 5 s^{-1} at 30 mM NaCl. The ratio of the amplitudes of the fast and slow components was approximately 9:1. The addition of an additional component did not improve the fitting. Thus, a two-component process was sufficient to describe this reaction, and all data of the present experiment were adequately fitted.

The stopped-flow experiments were performed with various concentrations of Cl^- or Br^- from 20 to 90 mM at 10 °C. Figure 6 shows rate constants (k) of the fast and slow components as functions of anion concentrations, since the rate constants of both the fast and slow phases are dependent on this concentration. The dependences of both rate constants on Br^- concentration were greater than those on Cl^-, similar to the K_d value (Table 1).

Figure 7 shows an Arrhenius plot of the rate constant for the fast phase between 10 and 30 °C. The values of ln k were linearly correlated with $1/T$. The apparent activation energy and frequency factor were calculated to be 35 and 30 kJ/mol and 18.5 and 16.4 s^{-1} for Cl^- and Br^- by the least-squares fitting, respectively. On the other hand, in an Arrhenius plot of the slow component, the data points were scattered and no systematic tendency was observed. This is

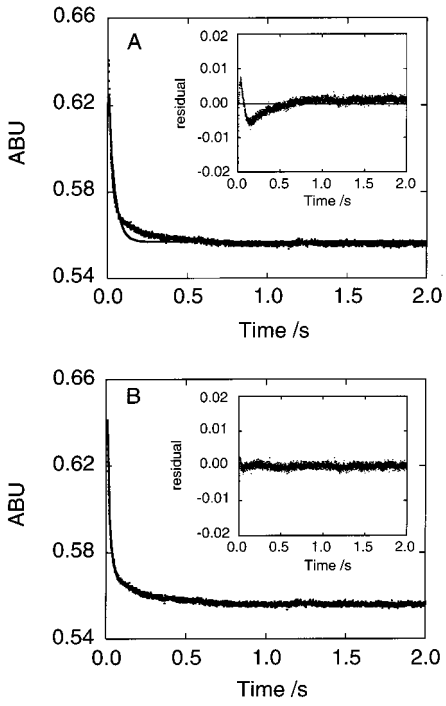

FIGURE 5: Absorption changes of *p*hR by stopped-flow rapid mixing with Cl^-. Traces were measured at 633 nm under the same conditions as those in Figure 4. The curves were fitted with (A) single-exponential and (B) two-exponential decay equations. Insets: difference between the observed and fitted curves.

presumably because the slow phase amounts to only 10% of the total absorption change and the kinetic constants obtained might not be sufficiently accurate for the Arrhenius analysis.

DISCUSSION

Expression and Purification of Histidine-Tagged phR. Halorhodopsin from *N. pharaonis* (*p*hR) was functionally expressed in *E. coli* using the method of Shimono et al. (*22*), and the *E. coli* expression system of *p*hR having a histidine tag at the C-terminus was as previously reported (*23*). In this work, the histidine-tagged region was introduced into the C-terminus of the protein.

^{1}MTETLP...TPADD^{291}**LE**HHHHHH (this work)

^{1}MTETLP...TPADD^{291}**GS**HHHHHH (previous work)

The present histidine-tagged proteins were expressed and purified with a yield up to 20 mg/L of cell culture. This yield was 30-fold greater than that reported previously (0.64 mg/L of cell culture), although the difference consisted only of the sequence at the C-terminal linker (LE instead of GS). The exact reason for the high yield is not known. The photocycling kinetics of the histidine-tagged *p*hR was compared with that of the wild-type *p*hR (*23*). The photocycles of these proteins showed similar kinetics. In addition, the photoactivity and affinity of the present recombinant *p*hR for Cl^- were the same as those of the authentic *p*hR (*20*). Moreover, the two phases of the Cl^- binding observed by the time-resolved absorption changes were also observed with the wild-type *p*hR (without the histidine tag). Thus, it is concluded that the histidine-tag modification at the C-terminus of *p*hR does not seriously affect the photoactivity

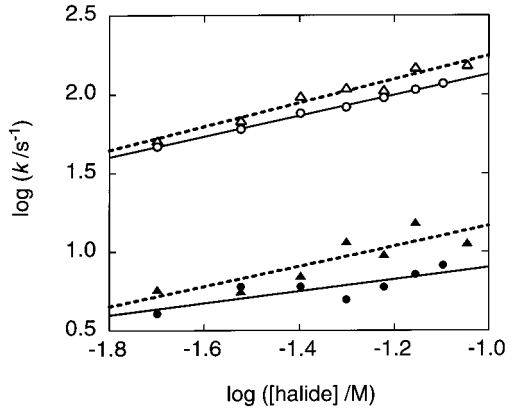

FIGURE 6: Plots of the logarithm of k vs logarithms of halide concentrations. The rate constants of the fast and slow phase are indicated by open and closed symbols, respectively. Data shown with triangles and dotted lines are for Br^-, while those shown with circles and solid lines are for Cl^-. The reaction was carried out at 10 °C.

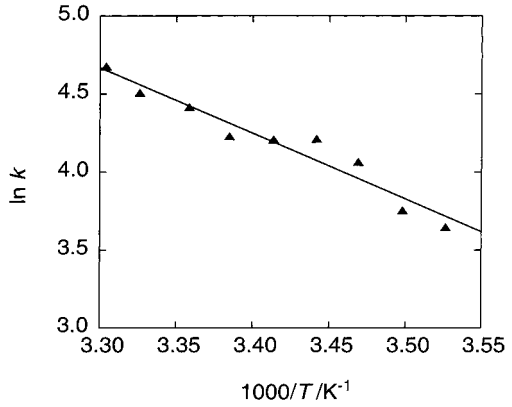

FIGURE 7: Arrhenius plot of the rate constants of the fast phase between 10 and 30 °C. The final NaCl concentration of the stopped-flow experiments was 20 mM.

and the anion uptake. This histidine tag affords a simple purification with a single column while the authentic *p*hR was purified using multistep chromatography.

Circular Dichroic Spectra of phR. Circular dichroic spectra of the authentic *p*hR before (blue form) and after (purple form) the addition of NaCl were observed in 0.1% DM and 10 mM citrate/phosphate buffer (pH 7.0) (*20*). Both forms exhibited a bilobe in the region of 450−700 nm with a crossover point at 575 nm for *p*hR and 595 nm for *p*hR^{blue}, which are approximately equal to the absorption maximum. On the basis of CD spectroscopic studies of bR, a bilobe in the visible region is interpreted as a superposition of the following two components: (1) symmetrical positive and negative bands arising from excitonic interaction between chromophores of neighboring molecules and (2) a positive band originating from the retinal pocket with its own asymmetric protein environment (*25*−*27*). Thus, even if molecular assembling or intermolecular orientation between chromophores has vanished (monomeric form), the positive band arising from the intramolecular interaction of the retinyl residue with the protein part should remain. Thus, the visible CD spectral pattern of bacterial rhodopsins is influenced by solubilized states with detergents. The ellipticity for hR purified from *H. salinarum* in 4 M NaCl with *n*-octyl β-D-glucopyranoside (octyl glucoside, OG) exhibited only a positive band, suggesting a monomeric form, but that solubilized with cholate exhibited a bilobe due to the oligomeric form (*28*). It has also been reported that the bilobe ellipticity of bR was reversibly decreased and increased by solubilizing with Triton X-100 and reconstituting with lipid, respectively (*29*). As shown in Figure 1, the present *p*hR with a histidine tag at the C-terminus exhibited an oligomeric form and symmetrical ellipticity for positive and negative bands under the Cl^--free condition. Upon addition of Cl^- to *p*hR^{blue}, the apparent ellipticity was increased in the positive band of the bilobe, while that in the negative band was unchanged. These findings suggest that Cl^- does not change the intermolecular interaction (the oligomeric state) and that Cl^- binding at the binding site [maybe near Arg-123 (Arg-108 for *s*hR)] changes the interaction of the retinal pocket with the surrounding amino acid residues. The increase of the positive band was also observed for Br^- and NO_3^-, with the exception of N_3^-, suggesting that the N_3^- anion interacts differently with amino acid residues from Cl^-, Br^-, and NO_3^- although N_3^- might be bound at the same site.

Anion Affinity of phR. The concentration dependence of the absorbance changes associated with the reaction of *p*hR^{blue} → *p*hR^X exhibited simple sigmoidal curves with the saturation for halides, Cl^- and Br^- (Figure 3). However, polyatomic anions, nitrate, and azide exhibited a steeper slope than that for halides. It was impossible to fit these saturation curves by assuming the presence of two individual binding sites. Thus, cooperativity for one binding site was introduced to obtain the curves best fitted to the Hill equation. Slightly cooperative binding of polyatomic anions was suggested from the Hill coefficients, as listed in Table 1. Scharf and Engelhard (*20*) previously analyzed saturation curves of the authentic *p*hR for the same halides and polyatomic anions at a slightly lower range of concentration than that of our study. Our results for halides essentially agree with their report. In the case of nitrate and azide, however, there was a slight difference for the slope of the saturation curve (Hill coefficient = 1.6). This difference may have arisen because our measurements cover the higher concentration range. The histidine tag has a slight effect on the Hill coefficient, but the binding behavior of the present histidine-tagged *p*hR is essentially the same as the authentic *p*hR or the *p*hR expressed in *E. coli* without the tag.

There are two models for the anion-binding sites of *s*hR. From spectroscopic analysis of the binding of different anions to *s*hR in Na_2SO_4, which itself does not bind to the protein, it was previously postulated that the anions occupied two different sites (*14*). One of these sites binds only polyatomic anions (site I), whereas the other (site II) is specific for anions such as Cl^-. Nitrate is able to bind to both sites. These two sites might participate in the uptake and the release of Cl^- during the transport. Other results from FTIR spectroscopy (*16*) indicated only one anion-binding site with two states. In addition, the high-resolution crystal structure of *s*hR (*10*) showed that *s*hR has one Cl^- in the chromophore, supporting the notion of one binding site with two states. Assuming the same Cl^- binding site (since the amino acid residues around the site are all conserved between *p*hR and *s*hR), there may be just one Cl^--binding site near the chromophore for *p*hR. The fact that the ΔA curve was well fitted with the Hill coefficient of about unity (Figure 3) supports the notion of one binding site. However, the presence of more than two

binding sites in hR, which do not directly interact with the chromophore, is undeniable based on the spectroscopic data. In fact, other binding sites with lower affinity were suggested using ^{35}Cl NMR (*17*) and electric current measurement (*19*, *30*). More detailed analysis is necessary to clear this problem.

Chloride Uptake of phR in the Dark. Chloride uptake and release of the authentic *p*hR during the photocycle were investigated in detail by Váró et al. (*7*). The photocycle has been described by the scheme hR → K ↔ L ↔ N ↔ O ↔ hR′ → hR. From the Cl^- dependences of the rate constants in this model, the N → O and O → hR′ reactions are considered as the steps in which Cl^- release and uptake occur, respectively. The rate constant of Cl^- uptake for the O → hR′ reaction was estimated to be 270 s^{-1} at 100 mM NaCl. The rate constant of the fast component of passive Cl^- diffusion from bulk to *p*hR^{blue} in the dark under the same conditions as those of the photocycling measurements was almost the same (260 s^{-1} at 100 mM NaCl). Moreover, Váró et al. (*7*) reported that the logarithm of the rate constants of the O → hR′ reaction (Cl^- uptake process during the photocycle) has a slope of 0.75 when plotted against the logarithm of Cl^- concentration. The origin of what appears to be a reaction order of 0.75 for the chloride binding has not been clear. However, in our study, it is worthwhile to note that the identical slope (0.7) for the logarithm of the rate constants of the fast component against the logarithm of Cl^- concentration was obtained in the uptake of Cl^- by *p*hR^{blue} in the dark (Figure 6), suggesting similarity of the Cl^- uptake process in the photocycle and in the dark.

In addition, the apparent activation energy from the Eyring plot of the O → hR′ reaction (Figure 7 in ref *7*), E_a, was estimated to be about 36 kJ/mol. Interestingly, the apparent activation energy (35 kJ/mol) of the fast component obtained in this study was in accordance with those of the process in which Cl^- is taken up and moved near the chromophore through the extracellular channel (EC) during photoreaction (O → *p*hR′ reaction). Thus, it is quite reasonable that the fast phase of the Cl^- binding may occur through EC and that the Cl^- uptake during the photocycle at O → *p*hR′ reaction is ruled by a passive process. Both the O-intermediate and *p*hR^{blue} lost the negative charge of Cl^- near the chromophore.

In the time-resolved absorption changes observed by stopped-flow rapid mixing, the slow component was only 10% of the total absorption change. In this case, the slow change arises from the subsequent conformational change or the retinal isomerization. It is known that the chromophore isomer distribution (all-*trans*/13-*cis* ratio) in the ground state of *p*hR was reported to be heterogeneous and the all-*trans*-retinal percentage is 80−76% in *p*hR^X (X = Cl or Br), while that of *p*hR^{blue} is decreased to 62% (*31*). This implies that, during the process of *p*hR^{blue} → *p*hR^X, the chromophore should perform the isomerization, and the ratio of the all-*trans* isomer to the total chromophore increases to 18% (Cl^-) or 14% (Br^-). The difference between the extinction coefficients of these two isomers might be very small, which in turn would mean that the amplitude of the slow component might be small. In the light/dark-induced isomerization of bR, it has been reported that the all-*trans* form has only a 10% larger extinction coefficient than the 13-*cis* form (*32*). A similar conformational change or isomerization of *p*hR may occur at the reaction of O → *p*hR′ → *p*hR during the photocycle. The rate constant of the *p*hR′ → *p*hR reaction was estimated to be 10-fold smaller than that of the preceding O → *p*hR′ reaction. Interestingly, the two-phase binding in this study also gave a similar ratio of the rate constants. On the basis of our results and the previous reports for *p*hR mentioned above, it is proposed that a single uptake process of Cl^- through EC occurs, followed by a conformational change or the retinal isomerization. On the other hand, there is a question that the slow kinetics in the dark might be contributed from the presence of the uptake from the reverse direction, i.e., from the cyctoplasmic channel (CP). The presence of retinal may hinder the Cl^- diffusion to the binding site (possibly near Arg-123, which is located in EC). This may account for the slow process and the small amplitude. However, the degree of contribution of this uptake to the slow kinetics is unknown.

Similar time-resolved studies of anion binding to *p*hR have been performed to discuss diffusion-controlled collision without absorption change and the following step with absorption change and to determine the intrinsic rate constants of reversible binding of anions (*33*). This study supports a single binding site in *p*hR as well as our result. In addition, a more recent analysis of the *p*hR photocycle has been published (*34*). In this report, fast equilibrium between anion-bound and anion-free states is proposed.

In this paper, the rate constants and the apparent activation energy for the reaction of *p*hR^{blue} to *p*hR^X were estimated using stopped-flow rapid mixing. They were very similar to the values of the O → *p*hR′ or O → *p*hR′ → *p*hR process during the photocycle. This finding might suggest that the Cl^--uptake process during the light-driven Cl^- transport may be ruled by simple and nonenergy diffusion through EC. At the N-decay to O, Cl^- is expelled to the intracellular side and 13-*cis*-retinal isomerizes to all-*trans*, which might afford the nonoccupied Cl^- binding site due to the reorientation of the dipole moment of N−H of the Schiff base. Chloride might diffuse to this binding site by a simple diffusion through EC. The driving force of the Cl^- release is not clear at present, although an opening of the CP channel, like that shown in bR, may be assumed (*35*, *36*).

ACKNOWLEDGMENT

The authors are very grateful to Kazumi Shimono, Masayuki Iwamoto, and Yuki Sudo for invaluable discussion and advice on the expression of histidine-tagged *p*hR in *E. coli* cells.

REFERENCES

1. Lanyi, J. K. (1990) *Physiol. Rev. 70*, 319−330.
2. Otomo, J., Tomioka, H., and Sasabe, H. (1992) *Biochim. Biophys. Acta 1112*, 7−13.
3. Soppa, J., Duschl, J., and Oesterhelt, D. (1993) *J. Bacteriol. 175*, 2720−2726.
4. Ihara, K., Umemura, T., Katagiri, I., Kitajima-Ihara, T., Sugiyama, Y., Kimura, Y., and Mukohata, Y. (1999) *J. Mol. Biol. 285*, 163−174.
5. Matsuno-Yagi, A., and Mukohata, Y. (1980) *Arch. Biochem. Biophys. 199*, 297−303.
6. Bivin, D. B., and Stoeckenius, W. (1986) *J. Gen. Microbiol. 132*, 2167−2177.
7. Váró, G., Needleman, R., and Lanyi, J. K. (1995) *Biochemistry 34*, 14500−14507.

8. Váró, G., Brown, L. S., Sasaki, H., Kandori, H., Maeda, A., Needleman, R., and Lanyi, J. K. (1995) *Biochemistry 34*, 14490−14499.
9. Lanyi, J. K., Duschl, A., Hatfield, G. W., May, K. M., and Oesterhelt, D. (1990) *J. Biol. Chem. 265*, 1253−1260.
10. Kolbe, M., Besir, H., Essen, L. O., and Oesterhelt, D. (2000) *Science 288*, 1390−1396.
11. Váró, G., Zimányi, L., Fan, X., Sun, L., Needleman, R., and Lanyi, J. K. (1995) *Biophys. J. 68*, 2062−2072.
12. Ogurusu, T., Maeda, A., and Yoshizawa, T. (1984) *J. Biochem. 95*, 1073−1082.
13. Schobert, B., and Lanyi, J. K. (1986) *Biochemistry 25*, 4163−4167.
14. Lanyi, J. K., Duschl, A., Váró, G., and Zimányi, L. (1990) *FEBS Lett. 265*, 1−6.
15. Pande, C., Lanyi, J. K., and Callender, R. H. (1989) *Biophys. J. 55*, 425−431.
16. Walter, T. J., and Braiman, M. S. (1994) *Biochemistry 33*, 1724−1733.
17. Falke, J. J., Chan, S. I., Steiner, M., Oesterhelt, D., Towner, P., and Lanyi, J. K. (1984) *J. Biol. Chem. 259*, 2185−2189.
18. Rüdiger, M., and Oesterhelt, D. (1997) *EMBO J. 16*, 3813−3821.
19. Okuno, D., Asaumi, M., and Muneyuki, E. (1999) *Biochemistry 38*, 5422−5429.
20. Scharf, B., and Engelhard, M. (1994) *Biochemistry 33*, 6387−6393.
21. Duschl, A., Lanyi, J. K., and Zimányi, L. (1990) *J. Biol. Chem. 265*, 1261−1267.
22. Shimono, K., Iwamoto, M., Sumi, M., and Kamo, N. (1997) *FEBS Lett. 420*, 54−56.
23. Hohenfeld, I. P., Wegener, A. A., and Engelhard, M. (1999) *FEBS Lett. 442*, 198−202.
24. Hasselbacher, C. A., Spudich, J. L., and Dewey, T. G. (1988) *Biochemistry 27*, 2540−2546.
25. Heyn, M. P., Bauer, P. J., and Dencher, N. A. (1975) *Biochem. Biophys. Res. Commun. 67*, 897−903.
26. Becher, B. and Ebrey, T. G. (1976) *Biochem. Biophys. Res. Commun. 69*, 1−6.
27. Ebrey, T. G., Becher, B., Mao, B., Kilbride, P., and Honig, B. (1977) *J. Mol. Biol. 112*, 377−397.
28. Duschl, A., McCloskey, M. A., and Lanyi, J. K. (1988) *J. Biol. Chem. 263*, 17016−17022.
29. Mukhopadhyay, A. K., Dracheva, S., Bose, S., and Hendler, R. W. (1996) *Biochemistry 35*, 9245−9252.
30. Bamberg, E., Hegemann, P., and Oesterhelt, D. (1984) *Biochim. Biophys. Acta 773*, 53−60.
31. Gerscher, S., Mylrajan, M., Hildebrandt, P., Baron, M. H., Müller, R., and Engelhard, M. (1997) *Biochemistry 36*, 11012−11020.
32. Maeda, A., Iwasa, T., and Yoshizawa, T. (1977) *J. Biochem. 82*, 1599−1604.
33. Chizhov, I., Greeves, M., Scharf, B., Hess, B., and Engelhard, M. (1995) *Biophys. J.* (Abstract Th-Pos432, Biophysical Society Meeting).
34. Chizhov, I., and Engelhard, M. (2001) *Biophys. J. 81*, 1600−1612.
35. Spudich, J. L., and Lanyi, J. K. (1996) *Curr. Opin. Cell Biol. 8*, 452−457.
36. Spudich, J. L. (1998) *Mol. Microbiol. 28*, 1051−1058.

BI011788G